

Conformal quantum mechanics of causal diamonds: Quantum instability and semiclassical approximation

H. E. Camblong,¹ A. Chakraborty,^{2,3} P. Lopez-Duque,⁴ and C. Ordóñez⁴

¹*Department of Physics and Astronomy, University of San Francisco,
San Francisco, California 94117-1080, USA*

²*Department of Physics, University of Houston. Houston, Texas 77024-5005, USA*

³*Institute for Quantum Computing,
University of Waterloo, Waterloo, ON, CAN*

⁴*Department of Physics, University of Houston, Houston, Texas 77024-5005, USA*

(Dated: July 26, 2024)

Abstract

Causal diamonds are known to have thermal behavior that can be probed by finite-lifetime observers equipped with energy-scaled detectors. This thermality can be attributed to the time evolution of observers within the causal diamond, governed by one of the conformal quantum mechanics (CQM) symmetry generators: the noncompact hyperbolic operator S . In this paper, we show that the unbounded nature of S endows it with a quantum instability, which is a generalization of a similar property exhibited by the inverted harmonic oscillator potential. Our analysis is semiclassical, including a detailed phase-space study of the classical dynamics of S and its dual operator R , and a general semiclassical framework yielding basic instability and thermality properties that play a crucial role in the quantum behavior of the theory. For an observer with a finite lifetime \mathcal{T} , the detected temperature $T_D = 2\hbar/(\pi\mathcal{T})$ is associated with a Lyapunov exponent $\lambda_L = \pi T_D/\hbar$, which is half the upper saturation bound of the information scrambling rate.

I. INTRODUCTION

Causal diamonds are double-coned-shaped regions with remarkably simple structures in spacetime that appear to exhibit thermal behavior in the absence of spacetime curvature. In a related paper [1], we show that this thermal character is specifically driven by the time evolution of observers constrained within the causal diamond. The usefulness of causal diamonds in enforcing the basic causal behavior of systems confined between a beginning point A and end point B (see Fig. 1) has been recognized for decades, with the associated

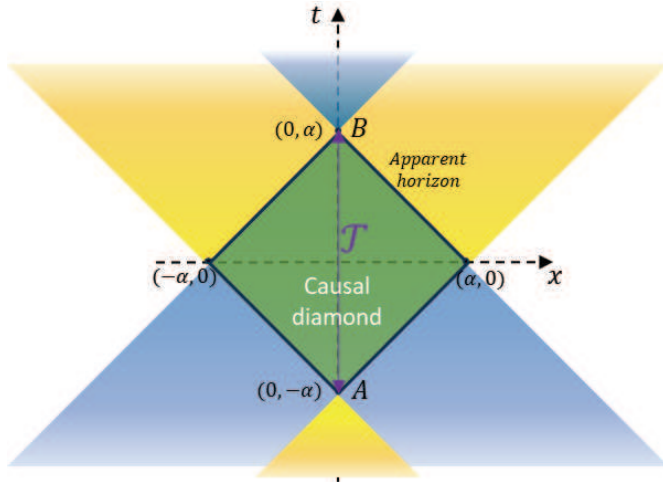


FIG. 1. The green region denotes the causal diamond of size 2α . The diamond's boundaries are causal horizons.

thermal effects first formally identified [2–4] with a conformally invariant vacuum subject to the Kubo-Martin-Schwinger (KMS) condition [5, 6]. A precise physical interpretation of this “diamond thermal effect” was advanced in Ref. [7] with the thermal time hypothesis [8], showing that they acquire a specific diamond temperature

$$T_D = \frac{\hbar}{\pi\alpha} , \quad (1)$$

where $\mathcal{T} = 2\alpha$ is the observer's lifetime (with 2α being the size of the diamond), and we will work in a system of units with $k_B = c = 1$. As displayed in Eq. (1), this is a quantum effect; moreover, it can be interpreted in terms of an energy-scaled detector [9], which, to a finite-lifetime “diamond observer,” makes the otherwise empty Minkowski background populated with particle excitations with a thermal density matrix. This concept was also discussed within an open quantum systems approach in Ref. [10], and the thermal interpretation

was verified and rediscovered in several works [11–16] using a variety of standard relativistic quantum techniques, including extensions to de Sitter spacetime [17, 18] and black holes [14, 19], and a description of relativistic quantum information and entanglement [20].

A. Spacetime, Horizons, and Quantum Information Scrambling

In essence, the diamond thermal effect can be interpreted as a consequence of the existence of apparent horizons (Fig. 1) that restrict causal access and yield emergent mixed states of thermal character. In this view, the physics of thermality exhibited by causal diamonds is analogous to that perceived by accelerated observers, i.e., the Fulling-Davies-Unruh effect [21–24], where a causal restriction applies with a Rindler horizon, leading to a thermal state of temperature $T_U = \hbar a / 2\pi$, where a is the observer’s acceleration in Minkowski spacetime. More generally, such thermal and thermodynamic effects are expected to be observed in all systems with horizons, including the paradigmatic Hawking effect [25–27] for black holes, which consists of the emission of thermal radiation with a temperature

$$T_H = \frac{\hbar\kappa}{2\pi}, \quad (2)$$

where κ is the black-hole surface gravity. In particular, the thermodynamics of black holes [28, 29] predicts a black hole entropy proportional to the horizon area [30, 31], and has signaled the crucial function of conformal symmetry in these systems.

Black holes appear to be the fastest information scramblers available in nature, given that the only information coming out of a black hole is thermal in nature [32]. As a result, interest in the physics of black-hole radiation and thermodynamics has seen a significant upsurge in recent years via its connection with quantum information theory and quantum chaos. In a recent seminal paper [33], it was argued that there exists a bound on the rate of growth of chaos in thermal quantum systems, which can be described as the information scrambling rate quantified by the out-of-time-order correlation (OTOC) function. This diagnostic tool for quantum chaos has become of widespread use in a variety of physical systems [34–38]; the OTOC can grow exponentially in a quantum chaotic system, with the information scrambling rate (quantum Lyapunov exponent) λ_L having the upper bound

$$\lambda_L \leq \frac{2\pi T}{\hbar}, \quad (3)$$

where T is the temperature of the system. For a black hole, the growth rate of information scrambling saturates the upper bound, so that $\lambda_L = 2\pi T_H/\hbar$, with T_H being the Hawking temperature. Hence, black holes can be considered as maximally chaotic quantum systems. Moreover, this led to the conjecture that the bound saturation of a system is the signature that it is holographic dual to a black hole [36, 39], with an example provided by the Sachdev-Ye-Kitaev (STK) model [40–43].

B. The Multiple Roles of Conformal Symmetry and Conformal Quantum Mechanics

The relevance of conformal symmetry for the thermal properties black holes has been a recurrent theme in fundamental physics, using a variety of approaches, e.g., Refs. [44, 45], [46, 47], [48], and [49]–[52]. More specifically, *conformal quantum mechanics (CQM)* [53] can be used to study black hole thermodynamics, including also their concomitant fast-scrambling nature. The CQM approach to black holes has been developed into a universal model of black hole entropy from near-horizon physics [54–57], and as the basis for the framework of black-hole acceleration radiation [58–61].

In this paper, we will use the dAAF model of CQM, as a $(0+1)$ -dimensional conformal field theory [53], which involves the action $S_{\text{CQM}}[Q] = \int dt \mathcal{L}_{\text{CQM}}(Q, \dot{Q})$, defined in terms of a field or generalized coordinate Q , with $P = \dot{Q}$ being its time derivative, and where the Lagrangian is

$$\mathcal{L}_{\text{CQM}} = \frac{1}{2}\dot{Q}^2 - \frac{g}{2Q^2}, \quad (4)$$

with $g > 0$ being a dimensionless coupling constant for the scale-invariant potential $g/2Q^2$. The action is invariant under time transformations that correspond to the conformal group $\text{SO}(2,1) \simeq \text{SL}(2, \mathbb{R})$ with generators that include the Hamiltonian H (time translations), the dilation operator $D = tH - (PQ + QP)/4$ (rescalings), and the special conformal operator $K = 2tD - t^2H + Q^2/2$ (translations of reciprocal time).

Independently from the more general applications of CQM to black hole thermodynamics, special cases of the CQM dilatation operator D have been recently used in a variety of problems [62] (in the context of the inverted harmonic oscillator). One particular form involves a scale-invariant xp -type potential that gives insights into quantum chaos [63, 64], and has been shown to exhibit a quantum instability that makes it useful as a near-horizon

probe of quantum information scrambling in black holes [65–71]. In our current paper, we will be using *similar physics, with a quantum instability, within the scope of the whole symmetry group of CQM as applied to causal diamonds.*

The applications mentioned above and of interest in this paper include black holes and related spacetime phenomena, including accelerated systems and finite-lifetime observers. However, it is noteworthy that CQM provides a versatile model to analyze a great variety of other physical systems in molecular physics [72–74], nanophysics [75], and nuclear and particle physics [75].

C. Goals and Outline

In this paper, we reveal additional aspects of the rich thermal physics of causal diamonds, as they arise from a quantum instability of the time evolution of diamond observers. We first study this instability using a semiclassical Hamiltonian approach, and then examine some corollaries within the semiclassical behavior that suggest thermality. This analysis is closely related to the recent findings concerning quantum instability and thermality driven by an inverted harmonic oscillator in black holes [65–71]. This construction is based on the property that the time evolution of a finite-lifetime observer is governed by an effective Hamiltonian [76, 77]: the CQM symmetry operator S , which is one of the noncompact generators of the conformal $\text{SO}(2,1)$ group in the original form of the dAFF model of CQM [53]. By the use of an analytic continuation that relates S with another generator of the $\text{SO}(2,1)$ group: the elliptic operator R [78], and representing these generators with *an inverse-square potential combined with inverted or regular harmonic oscillator*, we carry out a systematic semiclassical analysis based on the periodic orbits of R . This analysis highlights the following novel properties:

- The *thermal nature of a causal diamond can be attributed to the quantum instability caused by the S operator*. While this is analyzed semiclassically in this article, a more general framework can be developed via path-integral functionals [1, 78].
- The exploration of *instability and quantum chaos with CQM generators in spacetime physics* is thus extended from the dilation generator D to the broader set of $\text{SO}(2,1)$ symmetries of CQM.

- A consistent *paradigm of CQM symmetries being connected to instabilities and vacuum thermal effects* is thus developed, corroborating the insightful findings of Refs. [65–70] for black holes, within the simpler setting of causal diamonds in flat spacetime. This provides *insight into quantum scrambling relations* of the form of Eq. (3).

This article is structured as follows. In Sec. II, we consider the basic ingredients of CQM, its symmetry generators, along with operator dualities, and highlight their use for the time evolution within causal diamonds—additional details can be found in Ref. [1]. In Sec. III, we show the emergence of dynamical instability due to the time evolution with the CQM hyperbolic generator S . In Sec. IV, we explore additional aspects of the semiclassical behavior by using the CQM operator dualities via their analytic continuation; the results of this analysis suggest a thermal behavior at the diamond temperature T_D , Eq. (1), also providing other physical quantities, like the density of states. In Section V we conclude this work with a brief overview, context, and extensions of this research. Appendix A discusses the density of states using the CQM path-integral theory of Ref. [78], making contact with the predictions of the semiclassical regime.

II. SYMMETRY ALGEBRA OF CONFORMAL QUANTUM MECHANICS (CQM): OPERATOR DUALITIES AND RELATIONSHIP TO CAUSAL DIAMONDS

In what follows, unless stated otherwise, we will use units with $\hbar = 1$. The notation and conventions used in this paper are adopted from Refs. [1, 78]. This is a brief outline of the main relations needed for the semiclassical theory; detailed derivations can be found in Ref. [78], and additional information relevant for causal diamonds in Ref. [1].

A. CQM Symmetry Generators and Operator Duality

The dAAF model of CQM [53], defined by the action associated with the Lagrangian of Eq. (4), has an $SO(2,1)$ symmetry governed by the generators H, D and K as outlined in Sec. I. Given the comparable relevance of all three independent operators, one can consider the generalized linear combination $G = uH + vD + wK$ as a possible effective Hamiltonian in its own right. The discriminant $\Delta = v^2 - 4uw$ determines its nature as elliptic: $\Delta < 0$ (including R below), hyperbolic: $\Delta > 0$ (including D and S below), and parabolic:

$\Delta = 0$, (including H and K). In each family, the Hamiltonian representation of these operators is unique up to a proportionality constant. The modified canonical variables q and $p = \dot{q}$ are transformed by adopting G as an effective Hamiltonian, in the form $q(\tau) = Q(t)/|u + vt + wt^2|^{1/2}$ and $p = |f_G|^{1/2}(P - \dot{f}_G Q/2f_G)$, where $f_G(t) = u + vt + wt^2$, with the dot notation for derivatives with respect to the original time t , and with a corresponding effective time $d\tau = dt/(u + vt + wt^2)$ adapted to each operator [78].

Within this generalized framework, the operators H and K can be replaced by the additive/subtractive linear combinations commonly labeled by R and S ; these form the Weyl-Cartan basis [79], with a commutator algebra that identifies the symmetry structure for the $(0+1)$ -dimensional version of conformal field theory [80]. For our purposes, allowing for the following physical insight, we will use the rescaled versions

$$R = H + \frac{1}{\alpha^2} K = \frac{1}{2} p_{R,S}^2 + \frac{g}{2q_{R,S}^2} + \frac{1}{2\alpha^2} q_{R,S}^2 , \quad (5)$$

$$S = H - \frac{1}{\alpha^2} K = \frac{1}{2} p_{R,S}^2 + \frac{g}{2q_{R,S}^2} - \frac{1}{2\alpha^2} q_{R,S}^2 , \quad (6)$$

where α is an arbitrary parameter with dimensions of time. Remarkably, this CQM parameter α is geometrically determined to be the half-size of the causal diamond in our problem of interest (Fig. 1); see Sec. II B. In Eqs. (5)-(6), the field variables q and p are defined for each operator separately as $q_{R,S}$ and $p_{R,S}$ from the above formulas, with $\tau_{R,S}/\alpha = \tanh^{-1}(t/\alpha)$ and $\tan^{-1}(t/\alpha)$ respectively. Then, in the form (5)-(6), R and S admit a simpler physical interpretation as regular Hamiltonians with effective potentials

$$V_{R,S}(q) = \frac{g}{2q^2} \pm \frac{1}{2\alpha^2} q^2 , \quad (7)$$

which can be identified as a useful probe of their spectral properties. The effective potentials (7) consist of a sum of the inverse square potential and an inverted or regular harmonic oscillator potential, respectively. Thus, while the operator R is a modified harmonic oscillator, the operator S has a potential with a monotonic behavior and no lower or upper bounds. Figure 2 displays the form of the potential for the operator S , which is unbounded (from below and above). As a result, the elliptic and hyperbolic families are distinctly different: *elliptic operators are compact with a discrete spectrum, while hyperbolic operators are unbounded with a continuous spectrum*. However, these families are related by an *operator duality via analytic continuation of the parameter α* ; this can be seen directly from the form

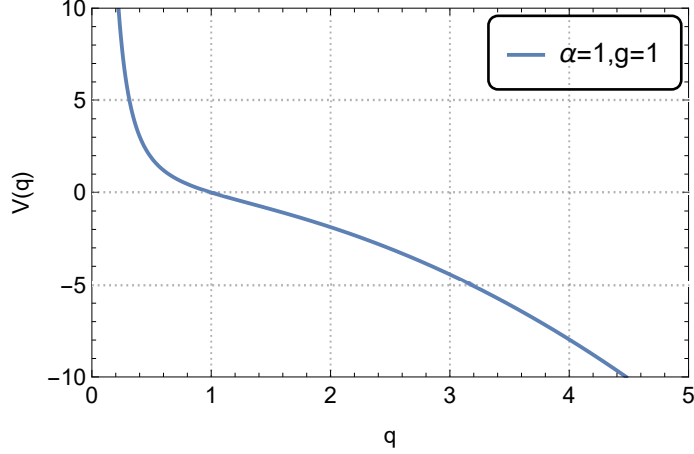


FIG. 2. Graph $V_S(q)$ vs q of the classical effective potential associated with the operator S . The chosen parameters are $g = 1$, $\alpha = 1$. The potential is monotonic with no lower or upper bounds, and has two competing behaviors: an effective centrifugal-like barrier for small q and an inverted harmonic oscillator behavior as $q \rightarrow \infty$.

of Eqs. (5) and (6) for their prototypical operators R and S via the analytic continuation [78]:

$$\begin{aligned} S &= R \left[\alpha_R^{-1} \longrightarrow \alpha_R^{-1} = -i\alpha_S^{-1} \right] \\ R &= S \left[\alpha_S^{-1} \longrightarrow \alpha_S^{-1} = i\alpha_R^{-1} \right] \end{aligned} \quad (8)$$

This is a useful transformation that permits the analysis of some properties of one operator family using the other one.

B. Dynamical Evolution of Diamond Observers via CQM

CQM is an exact, effective model for the dynamics in causal diamonds because *the operator S acts as an effective Hamiltonian* for time evolution [76, 77]. This conclusion can be elegantly deduced using radial conformal Killing fields (RCKF) [81], which, for the causal diamond, are generators of the $so(2, 1)$ algebra. The RCKF of this set that describes the time evolution of diamond observers is [76, 77]

$$S_K = \frac{1}{2\alpha} \left[(\alpha^2 - t^2 - r^2)\partial_t - 2tr\partial_r \right] \approx \frac{\alpha}{2i} S = \frac{\alpha}{2} \partial_\tau , \quad (9)$$

where ∂_t is the timelike Minkowski Killing vector, r is the radial distance from the origin, and the symbol \approx refers to the CQM-RCKF operator correspondence [1], which establishes an isomorphism between CQM as an effective theory and the actual physics of causal diamonds.

The integral curves of the RCKF operators S_K are timelike spacetime trajectories within the causal diamond. The statement $S_K \propto \partial_\tau$ indicates that this operator is the generator of time translations for a finite-lifetime observer whose proper time is τ . The time parameter τ associated with S is related to the original t (corresponding to H) in such a way the evolution via S with $\tau \in (-\infty, \infty)$ generates worldlines restricted to the causal diamond, with the inertial Minkowski time $t \in [-\alpha, \alpha]$.

III. INSTABILITY OF THE PHASE-SPACE DYNAMICS OF THE S OPERATOR: LYAPUNOV EXPONENT

This section develops one of the key novel results of our paper: *the phase-space dynamics of the hyperbolic operator S shows an instability behavior* that will subsequently appear to be related to the thermal properties of causal diamonds.

A. Hamiltonian Dynamics of the S Operator

The phase-space analysis is based on the identification of the operator S as the Hamiltonian for the time evolution governed by the natural time parameter τ_s , as was formulated in the previous section. The system's Hamiltonian dynamics can then be fully characterized using Hamilton's equation of motion,

$$\dot{q} = \frac{\partial S}{\partial p} , \quad \dot{p} = -\frac{\partial S}{\partial q} , \quad (10)$$

where $p = \dot{q}$ is the canonical conjugate momentum. Therefore, with the explicit form of the operator S in Eq. (6), Hamilton's equations read

$$\dot{q} = p , \quad \dot{p} = \frac{g}{q^3} + \frac{q}{\alpha^2} . \quad (11)$$

These equations are straightforward, but the behavior of the term q/α^2 in the second one has dramatic consequences for the stability analysis of the theory, as we show next.

B. Phase-Space Analysis of the S Operator: Lyapunov Exponent

The phase-space dynamics of the hyperbolic operator S can be understood by its representation with phase-space trajectories. These direction-field orbits are shown in Fig. 3,

with the asymptotes drawn in red.

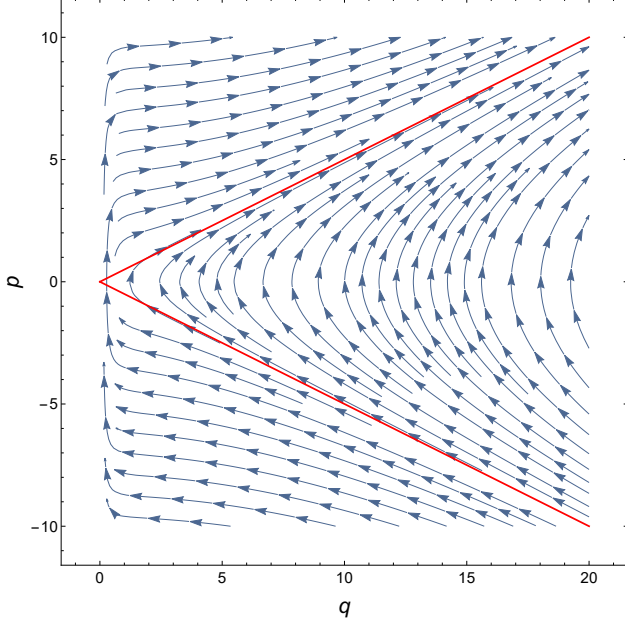


FIG. 3. Phase-space direction field for the trajectories for the S operator (with $g = 1, \alpha = 2$). The red line $p = q/\alpha$ shows the asymptotes of the trajectories.

An important property for our purposes is the nature of the stability of the phase-space orbits. This question can be answered by analyzing the evolution of a perturbation away from a given orbit. In particular, if the perturbation grows exponentially, then the orbit is unstable, with a Lyapunov exponent or instability factor λ_L defined as

$$\lambda_L = \lim_{\tau \rightarrow \infty} \frac{1}{\tau} \ln \left[\frac{\delta q(\tau)}{\delta q(0)} \right] . \quad (12)$$

For the phase-space orbits generated by the hyperbolic operator S , no obvious closed-form solution exists for all values of $\delta q(\tau)$. However, λ_L is completely determined by the long-term behavior of the perturbation $\delta(q)(\tau \rightarrow \infty)$. This asymptotic behavior can be determined via an effective-potential analysis, considering that S has a purely repulsive behavior, with an infinite barrier ($\propto 1/q^2$) near the configuration origin and an infinite well ($\propto -q^2$) near configuration infinity; thus, we expect that q will monotonically approach configuration infinity as τ gets larger. This asymptotic behavior sets in when $\tau \gg \alpha$ and $q^4 \gg g\alpha^2$, and reduces Eq. (11) self-consistently to

$$\dot{q} = p , \quad \dot{p} \approx \frac{q}{\alpha^2} , \quad (13)$$

which leads to the late-time perturbation

$$\delta q(\tau \gg \alpha) \Big|_{q^4 \gg g\alpha^2} \approx \delta q(0) e^{\tau/\alpha} . \quad (14)$$

As a result, the Lyapunov exponent is given by

$$\lambda_L = \frac{1}{\alpha} > 0 . \quad (15)$$

In conclusion, the positive instability factor characterizes a perturbation that grows exponentially in the q direction, as in Eq. (13), for any late-time orbit. This shows that the system is unstable, supporting the expected intuition for a potential dominated at late times by an inverted oscillator. This dynamical instability is closely related to the thermal behavior of causal diamonds, as we will see next.

IV. SEMICLASSICAL ASPECTS OF THERMALITY IN CAUSAL DIAMONDS

This section develops some of the properties of causal diamonds as they relate to the behavior of the CQM operators in the semiclassical regime. These properties hint at the existence of thermality in causal diamonds, *driven by the properties of the hyperbolic operator S as the generator of its time evolution*.

A. Semiclassical Analysis: Jacobi Action of R

The operator duality defined by the analytic continuation (8) permits an extrapolation of some results of R to operator S .

We start by considering closed periodic orbits γ of R in classical phase space. As shown in Ref. [1], these periodic orbits, despite being classical, are the ones used in quantum-mechanical traces in the path-integral formulation of the theory. As such, they encode the full-fledged quantum and thermal behavior, but the origin of this property can be probed at the semiclassical level. Moreover, they are the basic building blocks in the study of both classical and quantum chaos. In dealing with conservative systems, the existence of these orbits is guaranteed, leading to their definition via the Hamiltonian

$$R(q, p) = \frac{1}{2} p^2 + \frac{g}{2q^2} + \frac{1}{2\alpha_R^2} q^2 = E_\gamma , \quad (16)$$

for constant energy E_γ . In Eq. (16), we are denoting the Hamiltonian with the symbol of the corresponding generator $R \equiv \tilde{H}_R$; a typical trajectory of constant energy is shown in Figure 4.

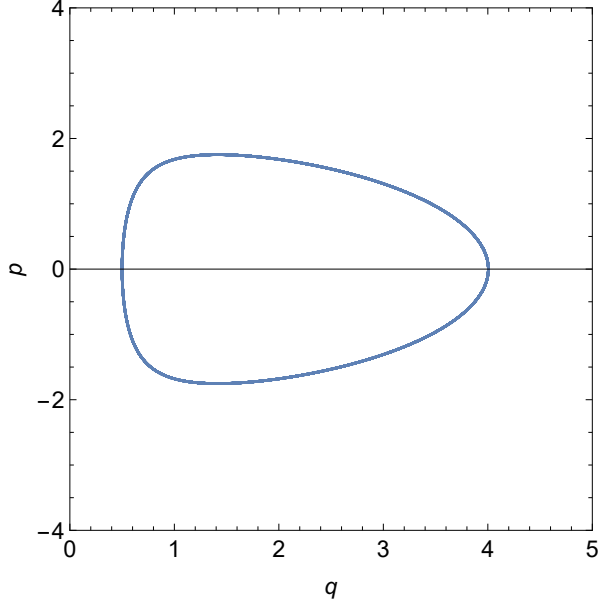


FIG. 4. Example of a closed trajectory for R (with $g = 1, \alpha = 2$, and $E_\gamma = 2$).

For the description of the orbits of the operator R defined by Eq. (16), a fixed-energy condition is required, and this converts the usual action $S[q; T]$ into the Legendre-transformed Jacobi action [1, 82–84]

$$W[q; E] = S[q; T] + ET \quad (17)$$

$$= \int pdq = \int \sqrt{2[E - V(q)]} dq, \quad (18)$$

where $V(q)$ is the potential defined in the usual manner, as in Eq. (7) or via Eq. (16). For the periodic orbits, the Jacobi action integral $W(E_\gamma)$ in Eq. (18) admits the following geometrical interpretation: it gives the area enclosed by the closed path in Fig. 4. For the R -Hamiltonian function in Eq. (16), it can be expressed in closed form as

$$\begin{aligned} W(E_\gamma) &= \oint p dq = \oint dq \sqrt{2E_\gamma - \frac{g}{q^2} - \frac{1}{\alpha_R^2} q^2} \\ &= \pi \alpha_R E_\gamma - \pi \sqrt{g} \end{aligned} \quad (19)$$

[e.g., 2.267.1 in Ref [85]]. The result of Eq. (19) shows that the Jacobi action is an increasing function with respect to α_R and decreasing with respect to g .

Finally, as Eq. (19) has been obtained via a classical argument, its correct semiclassical interpretation requires the *Langer correction* [86]: $\sqrt{g} \rightarrow \sqrt{g + 1/4} = \mu$, when used as part of the phase of a WKB or quasiclassical expansion in the presence of inverse square potential terms [54, 55]. Thus, the correct semiclassical result (to be used in Sec. IV C) is

$$W(E_\gamma)|_{\text{Langer-corr}} = \pi\alpha_R E_\gamma - \pi\mu . \quad (20)$$

B. Semiclassical Analysis: Microcanonical Approach and Information Scrambling

Equation (19) allows the computation of the period T_γ via the general equation for the Legendre-transformed conjugate classical transit time, $T = \partial W[q; E]/\partial E$. Thus, from Eq. (20), the time period T_γ of these closed orbits is

$$T_\gamma = \frac{\partial W(E_\gamma)}{\partial E_\gamma} = \pi\alpha_R . \quad (21)$$

An alternative semiclassical derivation of Eq. (21) is given in Appendix A, via the equivalent time-density relations, Eq. (A9).

The framework used in this section is microcanonical, i.e., for functionals of fixed energy E . In this setting, starting with the operator R and enforcing the analytic continuation of Eq. (8), the relation $\alpha_R = i\alpha_s = i\alpha$ is established, in such a way that the parameter value for operator R is the original geometrical parameter, i.e., $\alpha_s = \alpha$. Then, the time period T_γ can be rewritten in the form

$$T_\gamma|_{\text{microcanonical}} = T_R|_{\text{microcanonical}} = i\pi\alpha . \quad (22)$$

Two important corollaries are implied by the microcanonical result of Eq. (22). First, the period can be directly used in the calculation of the density of states $\rho(E)$; see Eq. (30) in the next section. Second, the output of Eq. (22) is an imaginary time when $\alpha_s = \alpha$ is real. This suggests that the system is in a thermal state, according to the correspondence between time and temperature in Euclidean field theory [87]. A rigorous interpretation of this result is given in Ref. [1] using the canonical ensemble. In essence, in the interpretation of the partition functions, and using the corresponding Euclidean time at the level of the path integrals, $\hbar\beta = T_{R_{\text{Eucl}}}|_{\text{canonical}} = \pi\alpha$, which implies an inverse temperature of a causal diamond given by

$$T_D^{-1} = \beta = \frac{\pi\alpha}{\hbar} , \quad (23)$$

in agreement with Eq. (1).

A final point is in order regarding the crucially important relationship of the diamond temperature (1) with the instability analysis of Sec. III, along with the related quantum information scrambling. The information scrambling rate λ_L for causal diamonds, according to Eq. (15), satisfies the upper-bound condition,

$$\lambda_L = \frac{1}{\alpha} < \frac{2\pi T_D}{\hbar} = \frac{2}{\alpha}, \quad (24)$$

with a strict inequality. This upper bound is determined by the observer's lifetime or diamond size, just as the upper bound for black holes is determined by the surface gravity. However, *unlike the case of black holes, the upper-bound is not saturated*. Most importantly, the main lesson from this analysis is that an instability is instrumental for nontrivial thermal and quantum information scrambling effects in spacetime, just as it was earlier found in Ref. [66] for black holes.

C. Semiclassical Framework and Gutzwiller Trace Formula

A general framework for the computation of the density of states—and more generally of all the functional integrals—is available within the semiclassical approximation. In the Gutzwiller approach [88, 89], which applies to the class of Hamiltonians of the form $p^2/2 + V(\mathbf{r})$, this is obtained via the asymptotic expansion of the path integral with respect to \hbar , leading to the semiclassical energy Green's function

$$G(\mathbf{r}'', \mathbf{r}'; E) = \overline{G}(\mathbf{r}'', \mathbf{r}'; E) + \sum_{\gamma} A_{\gamma}(\mathbf{r}'', \mathbf{r}'; E) \exp\left\{\left[\frac{i}{\hbar} \left(W_{\gamma}(\mathbf{r}'', \mathbf{r}'; E) - \mu_{\gamma} \frac{\pi}{2}\right)\right]\right\}. \quad (25)$$

In Eq. (25), the sum runs over all classical trajectories γ joining \mathbf{r}' to \mathbf{r}'' at given energy E but arbitrary times T , W_{γ} is the Jacobi action along the trajectory, μ_{γ} counts the number of points conjugate to \mathbf{r}' in energy, and the amplitude $A_{\gamma} = -\sqrt{D_{\gamma}}/[i\hbar(2\pi i\hbar)^{(d-1)/2}]$ enforces semiclassical probability conservation, with $D_{\gamma}(\mathbf{r}'', \mathbf{r}'; E)$ being the determinant of a Hessian matrix consisting of derivatives with respect to $\mathbf{r}'', \mathbf{r}'$, and E [90, 91]: In addition, $\overline{G}(\mathbf{r}'', \mathbf{r}'; E)$ is the contribution from the stationary point at $T = 0$ (singular part as $\mathbf{r}' \rightarrow \mathbf{r}''$) that yields the average density of states. This semiclassical Green's function provides not only the density of states, which is a standard tool for quantum chaos and stability analyses [92, 93], but also a more general approach to address all semiclassical questions. Careful evaluation

of the trace of Eq. (25) gives the Gutzwiller trace formula [88, 89], through [see Eq. (A4) and Refs. [1, 90, 91]]:

$$\rho(E) = -\frac{1}{\pi} \text{ImTr} \left[\hat{G}(E) \right] = \bar{\rho}(E) + \Delta\rho_{\text{sc}} , \quad (26)$$

where the Green's function trace,

$$\begin{aligned} \text{Tr} \left[\hat{G}(E) \right] &= \text{Tr} \left[\hat{\bar{G}}(E) \right] \\ &- \left(\frac{i}{\hbar} \sum_{\gamma_p} \sum_{k=1}^{\infty} \frac{T_{\gamma_p}}{\left| \det \left(M_{\gamma_p}^k - \mathbb{I} \right) \right|^{1/2}} \exp \left[\frac{i}{\hbar} k W(E_{\gamma_p}) - i \frac{m_{\gamma_p, k} \pi}{2} \right] \right) , \end{aligned} \quad (27)$$

is the critical functional in the microcanonical version of the theory. In Eqs. (26)–(27), both the trace and the density of states are given by the sum over all periodic orbits γ , including primitive orbits γ_p and their k -fold repetitions $k = 1, 2, \dots$, with T_γ being their corresponding periods; and

$$W(E_\gamma) = W(E_{\gamma_p, k}) = k W(E_{\gamma_p}) \quad (28)$$

is the closed-path Jacobi action. In addition, m_γ is the Maslov index for the trajectory (a modified extension of μ_γ); and M_γ is the monodromy matrix defined through the growth of a perturbation around the primitive orbit. The leading order $\bar{\rho}(E)$ is the “classical” density or Thomas-Fermi term discussed in the Appendix A; the other terms give an infinite sum: the semiclassical correction $\Delta\rho_{\text{sc}}$.

In this work, we are specifically interested in the time evolution dynamics generated by the hyperbolic operator S . As it is unbounded, it does not have any primitive orbits, and Eqs. (26)–(27) give no direct information. However, the analytic continuation of Eq. (8) extends it to the operator R , which does have closed orbits, as discussed in Sec. IV A; the results of that section provide the Jacobi action and the period, $W(E_\gamma)$ and T_γ , Eqs. (19)–(22). An analogous method has been previously used for the simpler inverted harmonic oscillator problem and the D operator of CQM [66]. Moreover, the Green's functions of the Euclideanized operator R give the same answers, properly extended, as those for operator S , according to [1]

$$G_{l+\nu}^{(R_{\text{Eucl}})}(r'', r'; E) \Big|_{\omega \rightarrow -i\omega} = G_{l+\nu}^{(S)}(r'', r'; E) , \quad (29)$$

where additional regularization may be in order; see Appendix A. Now, in the evaluation of Eq. (27) for the operator R , which involves an effective one-dimensional problem: for a given

energy, there is only one primitive periodic orbit, with period given by Eq. (22)—and this is already understood to be an analytic continuation, with an imaginary value. In addition, the Maslov indices are $m_{\gamma_p, k} = km_{\gamma_p}$, where the primitive Maslov index is $m_{\gamma_p} = 2$; and the monodromy matrix gives a trivial constant factor equal to one. Then, from Eq. (20), which reads $W(E_\gamma) \rightarrow W(E_\gamma)|_{\text{Langer-corr}} = \pi\alpha_R E_\gamma - \pi\mu\hbar$ with the Langer correction in standard units, the exponent in Eq. (27), with $\alpha_R = i\alpha_S = i\alpha$, becomes $ik[i\pi\alpha E/\hbar - \pi\mu - \pi]$, and the analytic continuation of the density of states of Eq. (26) takes the form

$$\begin{aligned}\rho^{(S)}(E) &= \bar{\rho}^{(S)}(E) + \text{Im} \left(\frac{i}{\pi\hbar} (i\pi\alpha) \sum_{k=1}^{\infty} e^{-ik\pi} \exp \left[k \left(-\pi\alpha \frac{E}{\hbar} - i\pi\mu \right) \right] \right) \\ &= \bar{\rho}^{(S)}(E) - \frac{\alpha}{\hbar} \text{Im} \left[\sum_{k=1}^{\infty} \left(-e^{-i\pi\mu} e^{-\pi\alpha E/\hbar} \right)^k \right].\end{aligned}\quad (30)$$

The semiclassical density of states of Eq. (30) consists of the Thomas-Fermi approximation average plus the semiclassical correction $\Delta\rho_{\text{sc}}$ [90], which is proportional to the corresponding terms in the pole-induced contribution of Eq. (A12) to the exact density of states—the extra factor of two is due to the addition from both $E > 0$ and $E < 0$ in the exact density of states (A11), which is an even function. This correction $\Delta\rho_{\text{sc}}$ consists of the k -fold repetitions that give a geometric series with ratio proportional to the Boltzmann factor $e^{-\beta E}$ at the diamond temperature, as follows by identification of the inverse temperature. The apparent or effective Boltzmann factor is subject to the following qualifications: (i) strictly speaking, a temperature dependence of a density of states is not a fully meaningful concept; (ii) the Boltzmann factor can be considered a sort of precursor or signal of the underlying thermal behavior in the form of thermal fluctuations in a bath at temperature T ; (iii) the expressions have to be properly regularized. But, most importantly, in a rigorous treatment of the system, the complete thermal behavior should be properly probed and identified with the canonical partition function (A1) or density matrix, as shown in Ref. [1]; indeed, an inverse Fourier transform of the terms in Eq. (30) yields a sum with simple poles at $T = i\pi\alpha k$, with k integer, which, by Mittag-Leffler's theorem [94], corresponds to the partition function (A1). It should be noted that, even though this is a one-dimensional problem, for which some aspects of the use of the Gutzwiller framework become trivial, an inverted oscillator generates a dynamic instability that still appears to lead to partially insightful information via the trace formula, Eqs. (26)–(27).

For comparison purposes and checks, comparable results for the density of states can be

found in Appendix A, using the exact Green's functions of Ref. [1].

V. DISCUSSION AND FURTHER WORK

We have explored some of the consequences of the CQM evolution in causal diamonds within the semiclassical limit. These results suggest thermality of the state detected by finite-lifetime observers, with the diamond temperature T_D of Eq. (1) driven by the time evolution via the S operator in CQM. This is essentially the analogous physics that has been studied in the gravitational background of a black hole, due to the presence of horizon effects [65–70].

More generally, it is known that the physics of CQM extends beyond the simplest version of the dAFF model. It also appears as a large- N limit of the Sachdev-Ye-Kitaev (SYK) model [40, 41], which is quantum chaotic in nature and finds other applications for black holes in AdS spacetime [42]. The links of the SYK model with chaos, and the bound of information scrambling, have recently become a promising research area, with possible connections and applications to a broad range of areas of physics [43]. It seems plausible that further connections of our line of work with the SYK model may provide additional insights into the links between CQM, chaos, and black hole thermodynamics.

This paper has been focused on the semiclassical regime, but otherwise yields similar findings to our more general framework using path integrals in Ref. [1]. We are currently investigating methods to establish a more direct and connection of quantum mechanical chaos with the S operator using fully quantum mechanical tools. As is well-known, the finite-temperature out-of-time-order correlation (OTOC) function is such a tool [34–38]; and it can be applied to the single particle operator S , e.g., following the footsteps of Ref. [95]. While the specific details of the calculations will be reported elsewhere, we found that, similar to the harmonic oscillator, the OTOC of the operator R is also sinusoidal in nature, and an analytic continuation would yield an exponentially growing OTOC for the operator S , again similar to the inverted harmonic oscillator potential. As the exponential growth of the OTOC has been argued to be one of the signatures of a quantum chaotic system, these additional results would corroborate the existence of the instability we obtained in Sec. III, and confirming quantum chaotic aspects of the operator S .

Finally, as pointed out in our related references, time-dependent Stark or Zeeman effects

are potential candidates [9] to probe the thermal physics of causal diamonds in what could possibly amount to critical tests of relativistic quantum information.

ACKNOWLEDGMENTS

This material is based upon work supported by the Air Force Office of Scientific Research under Grant No. FA9550-21-1-0017 (C.R.O., A.C., and P.L.D.). C.R.O. was partially supported by the Army Research Office (ARO), grant W911NF-23-1-0202. H.E.C. acknowledges support by the University of San Francisco Faculty Development Fund.

Appendix A: Density of States From the Exact Energy Green's Functions

This appendix provides all the basic results on the exact density of states corresponding to the operator S .

1. Partition Functions

In Ref. [1], the quantum-mechanical partition functions [90] were defined by considering periodic boundary conditions where $q(t'') = q(t')$. These are formal traces of the relevant operators. In particular, $\tilde{Z}^{(H)}(T) \equiv \text{Tr}[K^{(H)}(T)] \equiv \text{Tr} \left[e^{-i\hat{H}T/\hbar} \right] = \int dq' K^{(H)}(q', q'; T)$, for the propagator $K^{(H)}(T)$ of any candidate Hamiltonian operator H . Then, for the CQM operator S , the partition function was shown to be

$$\tilde{Z}_{l+\nu}^{(S)}(T) = \tilde{Z}_{l+\nu}^{(R_{\text{Eucl}})}(T) = \frac{e^{-\mu\omega T}}{2 \sinh \omega T} \quad (\text{A1})$$

(coincident with the Euclideanized version for the operator R). The symbol $l + \nu$ as subscript [1] refers to the angular momentum channels l in d dimensions, with $\nu = d/2 - 1$, and $\mu = \sqrt{(l + \nu)^2 + g}$ is the conformal index; the notation for the path-integrals functionals and procedures to handle the inverse square potential follow Refs. [1, 78, 96, 97].

2. Green's Functions and Density of States

Similarly, for the energy Green's functions, defined to satisfy the resolvent operator equation $G^{(\pm)}(E) = (E - \hat{H} \pm i0^+)^{-1}$, their trace is

$$\text{Tr} \left[\hat{G}_{l+\nu}^{(S)}(E) \right] = \frac{1}{i\hbar} \int_0^\infty dT e^{iET/\hbar} \tilde{Z}_{l+\nu}^{(S)}(T) = \frac{1}{i\hbar} \int_0^\infty dT e^{iET/\hbar} \frac{e^{-\mu\omega T}}{2 \sinh \omega T} \quad (\text{A2})$$

$$= \frac{1}{i\hbar\omega} \int_0^\infty dz e^{iEz/\hbar\omega} \frac{e^{-\mu z}}{2 \sinh z} \quad (\text{A3})$$

(assuming the retarded operators/functions with the plus sign), where $z = \omega T$ and Eq. (A1) was used.

In what follows, we will consider only the density of states expressions for the original dAFF model, which corresponds to an effective one-dimensional problem ($d = 1$). In that case, as considered in the main text, the conformal index is $\mu = \sqrt{g + 1/4}$, as used in the Langer-correction transition between Eqs. (19) and (20). Also, as discussed in Ref. [1], the net path-integral functionals for an effective one-dimensional problem restricted to the positive half-line by an inverse square potential are the same as their individual angular momentum components. In particular, $\hat{G}(E) = \hat{G}_{l+\nu}(E)$, so that the density of states is obtained from the retarded Green's functions via [1, 90, 91]

$$\rho(E) = -\frac{1}{\pi} \text{Im} \text{Tr} \left[\hat{G}(E) \right] = -\frac{1}{\pi} \text{Im} \text{Tr} \left[\hat{G}_{l+\nu}(E) \right] . \quad (\text{A4})$$

Then, with Eq. (A3), the density of states for the operator S has the form

$$\rho^{(S)}(E) = -\frac{1}{2\pi\hbar} \text{Im} \left[\frac{1}{i\omega} \int_0^\infty dz e^{iEz/\hbar\omega} \frac{e^{-\mu z}}{\sinh z} \right] = \frac{1}{2\pi\hbar} \text{Re} \left(\frac{1}{\omega} \int_0^\infty dz \frac{\exp[i(\eta + i\mu)z]}{\sinh z} \right) , \quad (\text{A5})$$

where $\eta = E/(\hbar\omega)$. In addition, according to the relation [1]

$$\text{Tr} \left[\hat{G}^{(R_{\text{Eucl}})}(E) \right] \Big|_{\omega \rightarrow -i\omega} = \text{Tr} \left[\hat{G}^{(S)}(E) \right] , \quad (\text{A6})$$

this density function can also be computed with the Euclideanized version of the R operator, giving exactly the same result, but it requires *taking the real part of Eq. (A5) after the analytic continuation is performed*.

Several useful properties of Eq. (A5) can be highlighted with the following procedure. First, the integral $I = \int dz F(z)$, where $F(z) = e^{i\zeta z} (\sinh z)^{-1}$, with $\zeta = \eta + i\mu$, can be evaluated as follows. Expanding the denominator via a geometric series of exponentials,

$F(z) = 2 \sum_{n=0}^{\infty} e^{-z[(1+2n)-i\zeta]}$, and integrating, Eq. (A5) yields

$$\rho^{(S)}(E) = \frac{1}{\pi\hbar} \operatorname{Re} \left(\frac{1}{\omega} \sum_{n=0}^{\infty} \frac{1}{[(2n+\mu+1)-i\eta]} \right). \quad (\text{A7})$$

The series (A7) explicitly displays the poles in the denominator, with respect to the energy parameter η , which occur at $\eta = -i(2n+\mu+1)$; with a rotation in the omega plane, $\omega \rightarrow i\omega$, these become the discrete eigenvalues of the R operator, as seen in Refs. [1, 78]. Comparison of Eq. (A1) with the definition of the partition function shows that [1], as expected, the partition function is related to Eq. (A7) via a Fourier transform.

3. Regularization and Semiclassical Limit of the Density of States

Another important property of Eq. (A7) for our discussion below is that it is divergent, thus requiring regularization. This is a serious technical problem of the density of states of the operator S , unlike the original amplitude functions (propagator and Green's functions), which results from the trace operation applied to the energy Green's function. In effect, in Eq. (A7), taking ω to be real in this parametrization, the series is divergent for the S operator in a manner similar to a harmonic series. This should not be surprising because the operator S is not of trace class [98]. Thus, all the expressions at the level of $\rho^{(S)}(E)$ are purely formal, and they require some form of regularization via a careful redefinition of the model.

Some hints of how regularization works for this problem can be revealed from the semiclassical approximation, related to various aspects of the analysis of Sec. IV. As a first step, by using the corresponding expression for the operator R , i.e., via $\hat{G}^{(R_{\text{Eucl}})}(E)$, the density of states is well-defined (as for a radial harmonic oscillator in the quantum-mechanical interpretation); this is easily verified by replacing $\omega \rightarrow i\omega$ in Eq. (A7) and then taking the real part. Now, the known classical limit of the density of states can be derived from integration in classical phase space, and is

$$\bar{\rho}(E) = \frac{1}{\pi\hbar} \int_{q_-}^{q_+} \frac{dq}{|p(q; E)/M|}, \quad (\text{A8})$$

where $p(q; E)$ is defined via Eq. (16), and the integral is between the turning points q_{\mp} . This is known as the Thomas-Fermi approximation, average, or Weyl term in the density of states [90, 91]; and it is completely general within the semiclassical approximation.

In addition, for an operator with classical periodic orbits of period $T(E)$, one can write

$$T(E) = 2 \int_{q_-}^{q_+} \frac{dq}{|p(q; E)/M|}, \text{ so that } \bar{\rho}(E) = \frac{1}{2\pi\hbar} T(E). \quad (\text{A9})$$

The final results for the operator R are thus obtained by straightforward integration, which gives $\bar{\rho}(E) = 1/(2\hbar\omega)$ and $T(E) = \pi/\omega$. It is noteworthy that the latter expression is identical to Eq. (21), and this integration procedure is an alternative way of deriving the period, which is central to our characterization of the thermal nature of causal diamonds. On the other hand, for the operator S , which has a potential with an inverted harmonic oscillator term, there is only one finite turning point (and the other limit is at infinity), and this causes a divergence in the density of states and transit time. Using these classical integral expressions, an obvious regularization procedure is *real-space cutoff regularization*, i.e., for a particle confined in a box of length L . Then, by direct integration in the classical limit of the operator S , one gets a logarithmic leading order

$$\bar{\rho}^{(S)}(E) \approx \frac{1}{\pi\hbar\omega} \ln \left(\sqrt{\frac{2M}{|E|}} \omega L \right), \quad (\text{A10})$$

which is the leading high-energy approximation, when $E \gg \hbar\omega$. This regularization technique has been used for the pure inverted harmonic oscillator [99].

Another powerful approach available for this problem, given the form of the series (A7), is a *digamma-function regularization* technique, which is usually stated as the replacement via the formal identity $\sigma(z) \equiv \sum_{n=0}^{\infty} 1/(n+z) = -\psi(z)$, where $\psi(z) \equiv \psi^{(0)}(z)$ is the digamma (psi) function [85, 100]. This procedure is based on the more basic formal identity (Eq. 5.7.6 in Ref [100]): $\sigma(z) \equiv \sum_{n=0}^{\infty} 1/(n+z) = -\psi(z) + C$ where $C = -\gamma + \sum_{n=0}^{\infty} 1/(n+1)$ is an infinite constant (including the finite Euler-Mascheroni constant γ), which can either be assumed to be removed by regularization subtraction or interpreted via a physical regularization technique such as the cutoff procedure mentioned above. Thus, Eq. (A7) becomes

$$\rho^{(S)}(E) = -\frac{1}{2\pi\hbar} \text{Re} \left(\frac{1}{\omega} [\psi((\mu+1-i\eta)/2) - C] \right), \quad (\text{A11})$$

defined up to an energy-independent constant C . While the details are beyond the scope of this work, these considerations give an idea of how to deal with the divergence problem, and Eq. (A11), properly interpreted, describes the physical density of states. In a more detailed treatment, one can use asymptotic methods, with a Dirichlet boundary condition at $q = L$,

to further interpret and determine the leading behavior as $L \rightarrow \infty$, for all energies E , and correspondingly adjust the path-integral propagators and Green's functions derived in Ref. [78]. One simple check of the correctness of this procedure is to extract the asymptotic limit $\eta \gg 1$ (i.e. $E \gg \hbar\omega$) using Stirling's series for the digamma function (Eq. 5.11.2 in Ref [100]): $\psi(z) \sim \ln z - 1/(2z)$, with $z = (1 - i\zeta)/2 \sim -i\eta/2$, whose real part in Eq. (A11) yields $\rho^{(S)}(E) \sim [1/(2\pi\hbar\omega)] \ln(2/|\eta|)$, which agrees with Eq. (A10) and fixes the ad-hoc constant via the cutoff-length L , with $C = -\ln[\hbar/(M\omega L^2)]$.

4. Density of States: Contribution from Poles and Semiclassical Regime

Even though Eq. (A5) is a formal expression that requires regularization, additional information can also be gathered from examination of the integral in the complex time T plane. In effect, the integrand $F(z)$ has poles on the imaginary axis, located at $z_k = i\pi k$, where k is an integer, with residues $R_k = (-1)^k e^{i\zeta z_k} = (-e^{-\pi\zeta})^k = (-e^{-i\pi\mu} e^{-\pi\eta})^k$. These poles give a sort of resonant contribution to the density in the form of a series of terms, with each one due to a conjugate point of the action in the path integral (in the stationary-phase evaluation within the semiclassical method; see Sec. IV C). For $E > 0$, these terms can be extracted by performing the integral in the complex plane with a counterclockwise contour comprised of the half real axis L_1 ($\text{Re}(z) \in [0, \infty)$), the upper-half imaginary axis L_2 ($\text{Im}(z) \in [0, \infty)$) traversed downwards circumventing the poles, and a circular path C_R of large radius $R \rightarrow \infty$ connecting them. As the integrand has no singularities in the first quadrant (excluding the boundary poles on the imaginary line), and as $\int_{C_R} F(z) dz = 0$ in the limit $R \rightarrow \infty$, it follows that the original integral (A5) along the half real axis L_1 can be computed with the integral $\int_{L_2} F(z) dz$ (traversed backwards up and including the poles along the path itself). Thus, with $\alpha = 1/\omega$, Eq. (A5) gives

$$\rho^{(S)}(E) = \frac{\alpha}{2\pi\hbar} \text{Re} \left[\pi i \left(\frac{R_0}{2} + \sum_{k=1}^{\infty} R_k \right) \right] + f(E) = \frac{\alpha}{2\hbar} \text{Im} \left(e^{\pi\zeta} + 1 \right)^{-1} + f(E), \quad (\text{A12})$$

where each pole $z_k = i\pi k$, with $k > 0$, yields half the usual residue amount (due to a circumventing half-circle), while $k = 0$ gives only a quarter of the usual amount. It is noteworthy that, for $E < 0$, a similar procedure involves a clockwise contour closed with an infinite circular path in the lower-half plane; and L_2 along the lower-half imaginary axis going through similar poles $z_k = i\pi k$, with $k = 0, -1, -2, \dots$: the outcome is a reversal in

the sign of the energy, i.e., this conforms to the even nature of the density of states that can be deduced from Eq. (A5). The resulting value of the density of states, Eq. (A12), for $E > 0$, consists of: (i) the pole contributions, forming a geometric series (with the displayed sum), which reproduce the semiclassical correction $\Delta\rho_{\text{sc}}$ of Sec. IV C; and (ii) an extra term $f(E)$, which is the Cauchy principal value of the integral along the imaginary axis, and includes the average density plus higher orders in the expansion. An interesting feature of Eq. (A12) is that it involves an infinite geometric series with ratio $-e^{-i\pi\zeta} = -e^{-i\pi\mu}e^{-\beta E}$, which is proportional to an effective Boltzmann factor $e^{-\beta E}$ at the diamond temperature, Eq. (1), as follows by identification of the inverse temperature $\beta = \pi\alpha$. These findings are discussed in the main text, Sec. IV C, in the context of a systematic semiclassical approximation.

[1] H. E. Camblong, A. Chakraborty, P. Lopez Duque, C. R. Ordóñez, Conformal quantum mechanics of causal diamonds: Time evolution and thermality via path integral functionals, preprint.

[2] J. J Bisognano and E. H. Wichmann, On the duality condition for a Hermitean scalar field, *J. Math. Phys.* **16**, 985 (1975); J. J Bisognano and E. H. Wichmann, On the duality condition for quantum fields, *J. Math. Phys.* **17**, 303 (1976).

[3] P. D. Hislop and R. Longo, Modular structure of the local algebras associated with the free massless scalar field theory, *Commun. Math. Phys.* **84**, 71 (1982)

[4] R. Haag, *Local Quantum Physics: Fields, Particles, Algebras* (Springer, Berlin, 1996).

[5] R. Kubo, Statistical-Mechanical Theory of Irreversible Processes. *J. Phys. Soc. Japan* **12**, 570 (1957).

[6] P. C. Martin and J. Schwinger, Theory of Many-Particle Systems. I, *Phys. Rev.* **115**, 1342 (1959).

[7] P. Martinetti and C. Rovelli, Diamond's temperature: Unruh effect for bounded trajectories and thermal time hypothesis, *Classical and Quantum Gravity*, **20**, 4919 (2003).

[8] A. Connes and C. Rovelli, Von Neumann algebra automorphisms and time thermodynamics relation in general covariant quantum theories, *Class. Quant. Grav.* **11**, 2899 (1994).

[9] D. Su and T. C. Ralph, Spacetime diamonds, *Phys. Rev. D*, **93**, 044023 (2016).

- [10] A. Chakraborty, H. E. Camblong, and C. R. Ordóñez, Thermal effect in a causal diamond: open quantum systems approach, *Phys. Rev. D*, **106**, 045027 (2022).
- [11] P. Martinetti, Conformal mapping of Unruh temperature, *Mod. Phys. Lett. A*, **24**, 1473 (2009).
- [12] H. Casini, M. Huerta, and R. C. Myers, Towards a derivation of holographic entanglement entropy, *JHEP* **05** (2011) 036.
- [13] D. Ida, T. Okamoto, and M. Saito, Modular theory for operator algebra in a bounded region of space-time and quantum entanglement, *Prog. Theor. Exp. Phys.* (**2013**), 083E03.
- [14] T. De Lorenzo and A. Perez, Light cone thermodynamics, *Phys. Rev. D*, **97**, 044052 (2018).
- [15] T. Jacobson and M. Visser, Gravitational thermodynamics of causal diamonds in (A)dS, *SciPost Physics*, **7** (2019).
- [16] J. Foo, S. Onoe, M. Zych, and T. C. Ralph, Generating multi-partite entanglement from the quantum vacuum with a finite-lifetime mirror, *New Journal of Physics*, **22**, 083075 (2020).
- [17] Y. Tian, De Sitter thermodynamics from diamonds's temperature, *JHEP* **06** (2005) 045.
- [18] M. R. R. Good, A. Zhakenuly, and E. V. Linder, Mirror at the edge of the universe: Reflections on an accelerated boundary correspondence with de Sitter cosmology, *Phys. Rev. D* **102**, 045020 (2020).
- [19] T. De Lorenzo and A. Perez, Light cone black holes, *Phys. Rev. D*, **99**, 065009 (2019).
- [20] H. E. Camblong, A. Chakraborty, P. Lopez-Duque, and C. R. Ordóñez, Entanglement degradation in causal diamonds, *Phys. Rev. D*, **109**, 105003 (2024).
- [21] S. A. Fulling, Nonuniqueness of Canonical Field Quantization in Riemannian Space-Time, *Phys. Rev. D* **7**, 2850 (1973).
- [22] P. C. W. Davies, Scalar production in Schwarzschild and Rindler metrics, *J. Phys. A* **8**, 609 (1975).
- [23] W. G. Unruh, Notes on black-hole evaporation, *Phys. Rev. D*, **14(4)**, 870 (1976)
- [24] P. C. W. Davies, S. A. Fulling, and W. G. Unruh, Energy-momentum tensor near an evaporating black hole, *Phys. Rev. D*, **13**, 2720 (1976).
- [25] S. W. Hawking, Black hole explosions?, *Nature*, **248(5443)**, 30-31. (1974)
- [26] S. W. Hawking, Particle creation by black holes, *Communications in Mathematical Physics*, **43(3)**, 199-220. (1975)
- [27] S. W. Hawking, Black holes and thermodynamics, *Physical Review D*, **13(2)**, 191. (1976)

- [28] R. M. Wald, The thermodynamics of black holes, *Living reviews in relativity* **4**, 1-44. (2001)
- [29] D. N. Page, Hawking radiation and black hole thermodynamics, *New Journal of Physics* **7**.1, 203. (2005)
- [30] J. D. Bekenstein, Black holes and the second law, *Lettere al Nuovo Cimento* **4**, 737-740 (1972).
- [31] J. D. Bekenstein, Black holes and entropy, *Physical Review D*, **7**, 2333 (1973).
- [32] Y. Sekino and L. Susskind, Fast Scramblers, *JHEP* **0810**, 065. (2008)
- [33] J. Maldacena, S. H. Shenker, and D. Stanford, A bound on chaos. *JHEP* **2016**, 106. (2016).
- [34] E. L. Hahn, Spin echoes, *Phys. Rev.* **80**, 580 (1950).
- [35] A. I. Larkin and Y. N. Ovchinnikov, Quasiclassical method in the theory of superconductivity, *Sov. Phys. JETP* **28**, 1200 (1969).
- [36] S. H. Shenker and D. Stanford, Black holes and the butterfly effect, *J. High Energy Phys.* **2014**, 67 (2014).
- [37] R. Fan, P. Zhang, H. Shen, and H. Zhai, Out-of-time-order correlation for many-body localization, *Sci. Bull.* **62**, 707–711 (2017).
- [38] B. Swingle, Unscrambling the physics of out-of-time-order correlators, *Nat. Phys.* **14**, 988–990 (2018).
- [39] S. H. Shenker and D. Stanford, Stringy effects in scrambling, *J. High Energy Phys.* **2015**, 1 (2015).
- [40] S. Sachdev and J. Ye, Gapless spin-fluid ground state in a random quantum Heisenberg magnet, *Phys. Rev. Lett.* **70**, 3339 (1993).
- [41] J. Maldacena, and D. Stanford, Remarks on the Sachdev-Ye-Kitaev model, *Phys. Rev. D* **94**, 106002 (2016).
- [42] K. Jensen, Chaos in AdS 2 holography, *Physical Review Letters*, **117**(11), 111601 (2016).
- [43] R. J. Lewis-Swan, A. Safavi-Naini, A. M. Kaufman, and A. M. Rey, Dynamics of quantum information, *Nat. Rev. Phys.* **1**, 627–634 (2019).
- [44] A. Strominger and C. Vafa, Microscopic origin of the Bekenstein-Hawking entropy. *Physics Letters B* **379**(1-4), 99 (1996).
- [45] A. Strominger, Black hole entropy from near-horizon microstates, *Journal of High Energy Physics* **1998**(02), 009 (1998).

[46] S. Carlip, Black hole entropy from conformal field theory in any dimension, *Phys. Rev. Lett.* **82**, 2828 (1999).

[47] S. Carlip, Symmetries, horizons, and black hole entropy, *Gen. Relativ. Gravit.* **39**, 1519 (2007).

[48] S. Ryu and T. Takayanagi, Holographic derivation of entanglement entropy from the anti-de sitter space/conformal field theory correspondence. *Physical Review Letters* **96(18)**, 181602. (2006)

[49] M. Guica, T. Hartman, W. Song, and A. Strominger, The Kerr/CFT correspondence, *Phys. Rev. D* **80**, 124008 (2009).

[50] A. Castro and F. Larsen, Near-extremal Kerr entropy from AdS2 quantum gravity, *J. High Energy Phys.* **12** (2009) 037.

[51] T. Hartman, W. Song, and A. Strominger, Holographic derivation of Kerr-Newman scattering amplitudes for general charge and spin, *J. High Energy Phys.* **03** (2010) 118.

[52] A. Castro, A. Maloney, and A. Strominger, Hidden conformal symmetry of the Kerr black hole, *Phys. Rev. D* **82**, 024008 (2010).

[53] V. de Alfaro, S. Fubini and G. Furlan, Conformal invariance in quantum mechanics, *Nuovo Cimento* **A34**, 569 (1976).

[54] H. E. Camblong and C. R. Ordóñez, Black hole thermodynamics from near-horizon conformal quantum mechanics, *Physical Review D*, **71(10)**, 104029 (2005).

[55] H. E. Camblong and C. R. Ordóñez, Semiclassical methods in curved spacetime and black hole thermodynamics, *Physical Review D*, **71(12)**, 124040 (2005).

[56] H. E. Camblong and C. R. Ordóñez, Conformal enhancement of holographic scaling in black hole thermodynamics: A near-horizon heat-kernel framework, *Journal of High Energy Physics*, **2007**, 099.

[57] H. E. Camblong and C. R. Ordóñez, Conformal Tightness of Holographic Scaling in Black Hole Thermodynamics, *Classical and Quantum Gravity* **30 (17)**, 175007 (2013).

[58] H. E. Camblong, A. Chakraborty, and Ordóñez, Near-horizon aspects of acceleration radiation by free fall of an atom into a black hole, *Physical Review D* **102 (8)**, 085010 (2020).

[59] A. Azizi, H. E. Camblong, A. Chakraborty, C. R. Ordóñez, and M. O. Scully, Acceleration radiation of an atom freely falling into a Kerr black hole and near-horizon conformal quantum mechanics, *Physical Review D* **104 (6)**, 065006 (2021).

[60] A. Azizi, H. E. Camblong, A. Chakraborty, C. R. Ordóñez, and M. O. Scully, Quantum optics meets black hole thermodynamics via conformal quantum mechanics. I. Master equation for acceleration radiation. *Physical Review D*, **104**(8), 084086 (2021).

[61] A. Azizi, H. E. Camblong, A. Chakraborty, C. R. Ordóñez, and M. O. Scully, Quantum optics meets black hole thermodynamics via conformal quantum mechanics: II. Thermodynamics of acceleration radiation, *Physical Review D*, **104**(8), 084085 (2021).

[62] V. Subramanyan, S. S. Hegde, S. Vishveshwara, and B. Bradlyn, Physics of the Inverted Harmonic Oscillator: From the lowest Landau level to event horizons, *Ann. Phys. (N.Y.)*, **435**, 168470 (2021).

[63] M. V. Berry, and J. P. Keating, $H = xp$ and the Riemann zeros. In *Supersymmetry and Trace Formulae*, pp. 355-367 (Springer, Boston, MA, 1999).

[64] G. Sierra, and J. Rodríguez-Laguna, $H = xp$ Model Revisited and the Riemann Zeros. *Physical Review Letters*, **106**(20), 200201. (2011)

[65] S. Dalui, B. R. Majhi, and P. Mishra, Presence of horizon makes particle motion chaotic, *Phys. Lett. B* **788**, 486 (2019).

[66] S. Dalui, B. R. Majhi, and P. Mishra, Horizon induces instability locally and creates quantum thermality. *Physical Review D*, **102**(4), 044006. (2020)

[67] S. Dalui, and B. R. Majhi, Near-horizon local instability and quantum thermality. *Physical Review D*, **102**(12), 124047. (2020)

[68] S. Dalui, and B. R. Majhi, Horizon thermalization of Kerr black hole through local instability. *Physics Letters B*, **826**, 136899. (2022)

[69] B. R. Majhi, Is instability near a black hole key for "thermalization" of its horizon?, *Gen. Rel. Grav.* **54**, 90 (2022).

[70] G. R. Kane and B. R. Majhi, Thermality of horizon through near horizon instability: a path integral approach, *Gen. Rel. Grav.* **55**, 125 (2023).

[71] P. Betzios, N. Gaddam, and O. Papadoulaki, Black holes, quantum chaos, and the Riemann hypothesis. *SciPost Physics Core*, **4**(4), 032. (2021)

[72] H. E. Camblong, L. N. Epele, H. Fanchiotti, and C. A. García Canal, Quantum anomaly in molecular physics, *Phys. Rev. Lett.* **87**, 220402 (2001).

[73] H. E. Camblong, L. N. Epele, H. Fanchiotti, C. A. García Canal, and C. R. Ordóñez, Effective field theory program for conformal quantum anomalies, *Phys. Rev. A* **72**, 032107 (2005).

- [74] H. E. Camblong and C. R. Ordóñez, Anomaly in conformal quantum mechanics: From molecular physics to black holes, *Phys. Rev. D* **68**, 125013 (2003)
- [75] H. E. Camblong and C. R. Ordóñez, Renormalization in conformal quantum mechanics, *Phys. Lett. A* **345**, 22 (2005).
- [76] M. Arzano, Conformal quantum mechanics of causal diamonds, *Journal of High Energy Physics*, **2020**, 1-14 (2020)
- [77] M. Arzano, Vacuum thermal effects in flat space-time from conformal quantum mechanics. *Journal of High Energy Physics*, **2021(7)**, 1-14 (2021)
- [78] H. E. Camblong, A. Chakraborty, P. Lopez Duque, C. R. Ordóñez, Spectral properties of the symmetry generators of conformal quantum mechanics: A path-integral approach. *J. Math. Phys.* **64**, 092302 (2023).
- [79] B. Wybourne, *Classical Groups for Physicists* (Wiley, New York, 1974).
- [80] P. Di Francesco, P. Mathieu, and D. Sénéchal, *Conformal Field Theory* (Springer, 1997).
- [81] A. Herrero and J. A. Morales, Radial conformal motions in Minkowski space-time, *J. Math. Phys.* **40**, 3499 (1999).
- [82] L. D. Landau and E. M. Lifshitz, *Course of Theoretical Physics, Vol. 1, Mechanics* (Butterworth-Heinemann, Oxford, 1976).
- [83] H. Goldstein, C. P. Poole, J. L. Safko, *Classical Mechanics*, 3rd ed. (Addison-Wesley, Reading, MA, 2002).
- [84] C. Lanczos, *The Variational Principles of Mechanics* (University of Toronto Press, Toronto, 1970).
- [85] I. S. Gradshteyn and I. M. Ryzhik, *Tables of Integrals, Series, and Products* (Academic Press, Boston, MA, USA, 2015).
- [86] R. Langer, On the connection formulas and the solutions of the wave equation, *Phys. Rev.* **51**, 669 (1937).
- [87] A. Zee, *Quantum Field Theory in a Nutshell*, 2nd ed. (Princeton University Press, Princeton, 2010), p. 289.
- [88] M. C. Gutzwiller, Periodic orbits and classical quantization conditions, *J. Math. Phys.* **12**, 343 (1971).
- [89] M. C. Gutzwiller, *Chaos in Classical and Quantum Mechanics* (Springer-Verlag, New York, 1990).

[90] H. Kleinert, Path Integrals in Quantum Mechanics, Statistics, Polymer Physics, and Financial Markets, 5th ed. (World Scientific, Singapore, 2009); and references therein.

[91] C. Grosche and F. Steiner, Handbook of Feynman Path Integrals (Springer-Verlag, Berlin, 1998); and references therein.

[92] F. Haake, S. Gnutzmann, and M. Kuś, Quantum Signatures of Chaos, 4th ed. (Springer Nature Switzerland AG, 2018).

[93] H.-J. Stöckmann, Quantum Chaos: An Introduction (Cambridge University Press, Cambridge, 1999).

[94] L. Ahlfors, Complex analysis, 3rd ed. (McGraw Hill, New York, 1979).

[95] K. Hashimoto, K. Murata, and R. Yoshii, Out-of-time-order correlators in quantum mechanics, *Journal of High Energy Physics*, **2017**(10), 1-31 (2017)

[96] H. E. Camblong and C. R. Ordóñez, Path Integral Treatment of Singular Problems and Bound States, *Int. J. of Mod. Phys. A* **19**, 1413 (2004).

[97] H. E. Camblong and C. R. Ordóñez, Regularized Green's function for the inverse square potential, *Mod. Phys. Lett. A* **17**, 817 (2002).

[98] J. B. Conway, A Course in Operator Theory (American Mathematical Society, Providence, RI, 2000).

[99] G. Barton, Quantum mechanics of the inverted oscillator potential, *Ann. Phys. (N.Y.)* **166**, 322 (1986).

[100] F.W. J. Olver, D. W. Lozier, R. F. Boisvert, and C. W. Clark, NIST Handbook of Mathematical Functions (Cambridge University Press, Cambridge, England, 2010).